MITSUBISHI ELECTRIC RESEARCH LABORATORIES
http://www.merl.com

Quantification of Rolling-Element Bearing Fault Severity of Induction Machines

Zhang, Shen; Wang, Bingnan; Kanemaru, Makoto; Lin, Chungwei; Liu, Dehong; Habetler, Thomas

TR2019-033 June 25, 2019

Abstract

The characteristic frequencies of different types of bearing faults can be calculated by a well-defined frequencybased model that depends on the motor speed, the bearing geometry and the specific location of a defect inside a bearing. Therefore, the existence of a bearing fault as well as its specific fault type can be readily determined by performing frequency spectral analyses on the monitored signals. However, this traditional approach, despite being simple and intuitive, is not able to identify the severity of a bearing fault in a quantitatively manner. Moreover, it is often tedious and time-consuming to apply this approach to electric machines with different power ratings, as the bearing fault threshold values need to be manually calibrated for each motor running at every possible speed and carrying any possible load. This paper thus proposes a quantitative approach to estimate a bearing fault severity based on the air gap displacement profile, which is reconstructed from the mutual inductance variation profile estimated from a novel electrical model that only takes the stator current as input. In addition, the accuracy of the electrical model and the estimated bearing fault severity are validated by simulation results. The proposed method can be used to monitor bearing faults in induction machines with any power ratings that operate under any speeds and loads, and a bearing fault alarm will be triggered if the fault severity exceeds a universal threshold value.

International Electric Machines & Drives Conference (IEMDC)

Quantification of Rolling-Element Bearing Fault Severity of Induction Machines

Shen Zhang*‡, Bingnan Wang*, Makoto Kanemaru†,
Chungwei Lin*, Dehong Liu*, Koon Hoo Teo*, and Thomas G. Habetler‡
*Mitsubishi Electric Research Laboratories, 201 Broadway, Cambridge, MA 02139, USA
†Advanced R&D Center, Mitsubishi Electric Corporation, Amagasaki, Japan
‡School of Electrical and Computer Engineering, Georgia Institute of Technology, Atlanta, GA 30332, USA

***Abstract*—The characteristic frequencies of different types of bearing faults can be calculated by a well-defined frequency-based model that depends on the motor speed, the bearing geometry and the specific location of a defect inside a bearing. Therefore, the existence of a bearing fault as well as its specific fault type can be readily determined by performing frequency spectral analyses on the monitored signals. However, this traditional approach, despite being simple and intuitive, is not able to identify the severity of a bearing fault in a quantitatively manner. Moreover, it is often tedious and time-consuming to apply this approach to electric machines with different power ratings, as the bearing fault threshold values need to be manually calibrated for each motor running at every possible speed and carrying any possible load. This paper thus proposes a quantitative approach to estimate a bearing fault severity based on the air gap displacement profile, which is reconstructed from the mutual inductance variation profile estimated from a novel electrical model that only takes the stator current as input. In addition, the accuracy of the electrical model and the estimated bearing fault severity are validated by simulation results. The proposed method can be used to monitor bearing faults in induction machines with any power ratings that operate under any speeds and loads, and a bearing fault alarm will be triggered if the fault severity exceeds a universal threshold value.**

***Index Terms*—Bearing fault, fault severity, analytical model, mutual inductance variation, air gap displacement.**

I. Introduction

Induction machines are broadly used in various industry applications that include pumps, chemical, petrochemical, electrified transportation systems, etc. In many applications, these machines are operated under unfavorable conditions, such as high ambient temperature, high moisture and overload, which can eventually result in motor malfunctions that lead to high maintenance costs and unexpected downtime [1]–[3].

The malfunction of induction machines can be generally attributed to various faults of different categories, which include the drive inverter failures, stator winding insulation breakdown, broken rotor bar faults, as well as bearing faults and air gap eccentricity. Several surveys regarding the likelihood of induction machines failures conducted by the IEEE Industry Application Society (IEEE-IAS) [4]–[6] and the Japan Electrical Manufacturers' Association (JEMA) [7] reveal that a bearing fault is the most common fault type that accounts for 30% to 40% of the total faults.

Therefore, bearing fault detection has attracted the attention of many researchers and engineers from both mechanical engineering and electrical engineering. Specifically, this problem is approached by interpreting a variety of signals, including vibration, acoustic noise, and stator current, etc. The existence of a bearing fault as well as its specific fault type is readily determined by performing frequency spectral analyses on the monitored signals and analyzing the components at the characteristic fault frequencies, which can be calculated by a well-defined model [8] that depends on the motor speed, the bearing geometry and the location of a bearing defect.

However, monitoring the vibration or acoustic noise signals requires additional sensors that add to the system cost, or they can even become unfeasible to install due to space constraints. In addition, the fault detection accuracy can be also affected by background vibration or noise. Despite the advantages such as economic savings and simple implementation, stator current signature analysis can also encounter many practical issues. For example, the magnitude of stator currents at bearing fault signature frequencies can vary at different loads, speeds, and power ratings of the motors themselves, thus bringing challenges to identify the threshold stator current values to trigger a fault alarm at an arbitrary operating condition. Therefore, a thorough and systematic testing is usually required while the motor is still at the healthy condition, and the healthy data would be collected while the targeted motor is running at different load and speed. Moreover, this process, also referred to as the "Learning Stage" in [10], needs to be repeated for any motor with a different power rating, thus demanding heavy dataset to detect even nonfatal faults. In addition, the detection of bearing faults is mostly performed in a qualitative manner, whereas the exact faulty condition cannot be quantified. Therefore, there is a strong demand for a diagnostic method that is universal and accurate to quantify bearing faults with any power ratings and operating under any possible speed and load conditions.

In this context, this paper proposes a methodology to estimate the bearing fault severity in terms of radial air gap displacement by first developing a novel analytical model of an induction machine with bearing faults. The model is based on the transient partial differential equations of the induction machines, and it describes a relationship between the variations of mutual inductance induced by the bearing faults, as well as the corresponding changes of stator current. Using either the first-order or a series of Fourier Series

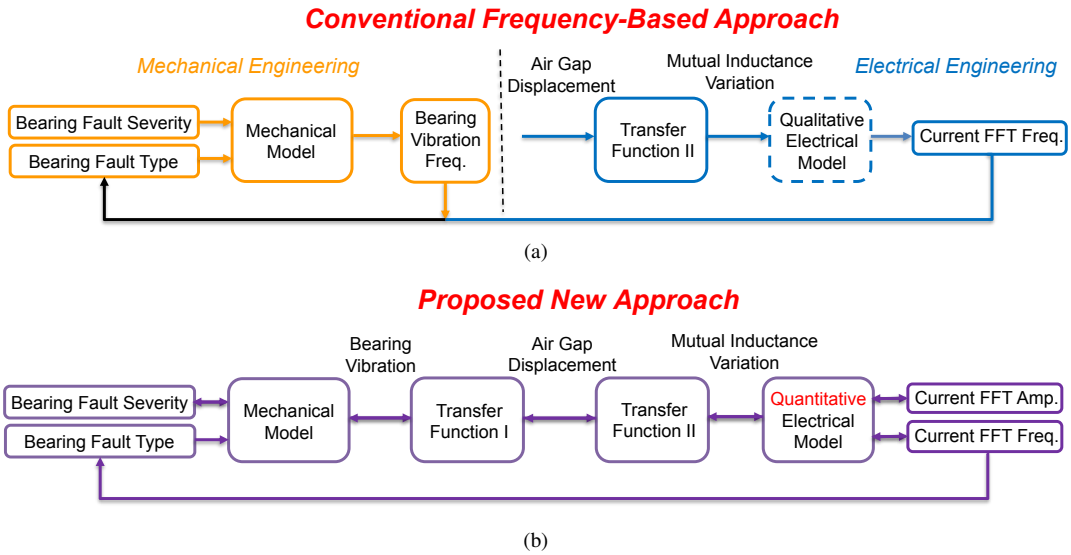

Fig. 1. Flow diagrams of bearing fault diagnostics (a) the traditional approach and (b) a new vision.

terms, the cumulative mutual inductance variation profile in the time domain can be reconstructed. The frequencies of the base cosine functions are multiples of the characteristic bearing fault frequency, and their amplitudes are determined by the faulty current through the proposed analytical model. Later, a transfer function is adopted to express the relationship between the mutual inductance variations and the air gap length variations, which is defined as a measure of the bearing fault severity in this study. The proposed mechanism enables a generalized and convenient bearing fault detection for induction machines with any power ratings and operating under arbitrary speeds and loads, and the fault alarms will be triggered if the estimated bearing fault severity exceeds a universal, predefined maximum tolerable bearing fault severity.

II. A New Vision for Bearing Fault Detection

A. Traditional Bearing Fault Detection Techniques

Fig. 1(a) is a flow diagram of the procedures undertaking by mechanical and electrical engineers to detect the presence of a bearing fault and its fault type. From the physical point of view, when a bearing fault appears on certain locations that characterizes its bearing fault type with a certain fault severity, some periodic vibration pulses will be generated as a result of the impacts between the rolling elements and the bearing raceways with a characterization frequency f_c solely determined by its fault type, which includes a cage defect hitting the inner/outer bearing raceways, an inner/outer raceway defect hitting the rolling elements, and a rolling element defect hitting both the inner and outer raceways. The mechanical mechanism for generating such vibrations can be constructed as a mechanical model [12], which is typically described with analytical equations [13] or finite element analysis [14]. While the relationship between a bearing fault type and its associated vibration frequency is already well-defined in Ref. [8], mechanical engineers have been investigating how the shape and intensity of vibration signals would change with respect to bearing defects of different width, depth and location. The vibration signals from a bearing fault can induce a periodic air gap displacement in the radial direction, which further causes a periodic variation of the mutual inductance L_m of the same characteristic fault frequency f_c according to Transfer Function II. Due to this mutual inductance change, the frequency component of the stator current at $|f_s \pm n \cdot f_c|$ will be present in response to the bearing fault, where f_s is the fundamental frequency of the input voltage. This mechanism can be formulated as a Qualitative Electrical Model, e.g., [9], which can identify the presence of a bearing fault and its fault type. However, this traditional approach is not able to predict the size or severity of such a bearing fault, either from vibration signals or from stator current signals.

B. A New Vision of Bearing Fault Detection

Fig. 1(b) is another flow diagram of a new vision proposed in this paper to estimate both the bearing fault type and fault severity with the integration of both electrical and mechanical models. The only input would be the extracted faulty current amplitudes of fault frequency f_c determined by the bearing geometry and the instantaneous motor speed [8]. Then the mutual inductance variation profile can be reconstructed with the developed Quantitative Electrical Model of induction machines with bearing faults, which can be further transformed into an air gap displacement signal with a Transfer Function II. With the knowledge of the bearing mounting positions on the shaft relative to the center of the air gap, the vibration intensity at the bearing locations can be inferred by a Transfer Function I based on either complex beam theories or simple linear decay functions of mechanical vibrations. The Mechanical Model can be constructed as direct analytical relationships between vibration signal pattern and bearing fault size/severity [13], or perform reverse mapping with finite element analysis

[14] for bearing defects with irregular shapes and thus its corresponding analytical equations are difficult to formulate. Similarly, the type of a bearing fault can be directly inferred from its associated faulty current frequency.

Compared to the traditional approach illustrated in Fig. 1(a), this new vision is an integrated approach of mechanical and electrical modeling. While the traditional approach can only determine the type of a bearing fault, this new vision can also estimate the actual fault severity. In addition, the proposed vision is nonintrusive as only the stator current information is used, and there is no need to install additional sensors such as the vibration and acoustic emission sensors.

This paper fulfills the electrical parts of this vision, namely the Quantitative Electrical Model and the transfer functions, and later determines the bearing fault severity in terms of the normalized air gap displacement estimated from the stator current. However, the final goal of this vision is to predict the size and location of a defect inside a bearing by only measuring and interpreting the stator current.

III. The Quantitative Electrical Model Estimating the Mutual Inductance Variation

The Quantitative Electrical Model is developed to estimate the mutual inductance variation from the input faulty current. The response to bearing faults can be considered as a combination of the mutual inductance variations due to the induced dynamic air gap eccentricity and the load torque oscillations due to the bearing defect that would further lead to speed oscillation. For most induction machine setups, however, the system inertia is large enough to suppress speed oscillations, and thus the effect of load torque oscillations is neglected in the later model development stage.

The mathematical model for the squirrel-cage induction machines in an arbitrary reference frame with an angular frequency ω_c can be expressed as

$$\begin{cases} u_{ds} = R_s i_{ds} + p\lambda_{ds} - \omega_c \lambda_{qs} \\ u_{qs} = R_s i_{qs} + p\lambda_{qs} + \omega_c \lambda_{ds} \\ 0 = R_r i_{dr} + p\lambda_{dr} - (\omega_c - \omega_r)\,\lambda_{qr} \\ 0 = R_r i_{qr} + p\lambda_{qr} + (\omega_c - \omega_r)\,\lambda_{qr} \end{cases} \tag{1}$$

$$\begin{cases} \lambda_{ds} = L_s i_{ds} + L_m i_{dr} \\ \lambda_{qs} = L_s i_{qs} + L_m i_{qr} \\ \lambda_{dr} = L_m i_{ds} + L_r i_{dr} \\ \lambda_{qr} = L_m i_{qs} + L_r i_{qr} \end{cases} \tag{2}$$

where u is the input voltage, R and L are the motor resistance and inductance, ω is the angular frequency, λ is the flux linkage, p is the differential operator, while the subscripts d and q represent the direct and quadrature axes, and the subscripts s, r and m denote the stator, rotor, and their mutual electromagnetic correlation.

Then a matrix form of the above equation can be written in (3), where U is the input matrix, $\hat{L}_1^{(0)}$ is the parametric matrix for a healthy induction machine, $X^{(0)}$ is the response matrix in the steady-state containing all the state variables of the stator and rotor flux linkages and currents, and K is the coefficient matrix for the first-order derivatives of the state variables X.

Similar to a small signal representation of equations (1) to (3) [15], consider a bearing fault that leads to a periodic air gap variation, which further leads to a periodic change of the mutual inductance. While the pattern of the periodic air gap variation can be decomposed into a series of Fourier Series, the simplest form is to only take its fundamental frequency component at f_c and its magnitude as ΔL_{m1}. The model can be formulated with this assumption first, and the final result of mutual inductance variation would be the superposition of all the harmonic contents derived in the same manner from this model. In this scenario, the updated mutual inductance is

$$L_m^{new} = L_m + \Delta L_{m1} \cos(w_{fc} t) \tag{4}$$

$$\underbrace{\begin{bmatrix} u_{ds} \\ u_{qs} \\ 0 \\ 0 \\ 0 \\ 0 \\ 0 \\ 0 \end{bmatrix}}_{U} = \underbrace{\begin{bmatrix} 0 & -w_c & 0 & 0 & R_s & 0 & 0 & 0 \\ w_c & 0 & 0 & 0 & 0 & R_s & 0 & 0 \\ 0 & 0 & 0 & -(w_c - w_r) & 0 & 0 & R_r & 0 \\ 0 & 0 & (w_c - w_r) & 0 & 0 & 0 & 0 & R_r \\ -1 & 0 & 0 & 0 & L_s & 0 & L_m & 0 \\ 0 & -1 & 0 & 0 & 0 & L_s & 0 & L_m \\ 0 & 0 & -1 & 0 & L_m & 0 & L_r & 0 \\ 0 & 0 & 0 & -1 & 0 & L_m & 0 & L_r \end{bmatrix}}_{\hat{L}_1^{(0)}} \cdot \underbrace{\begin{bmatrix} \lambda_{ds} \\ \lambda_{qs} \\ \lambda_{dr} \\ \lambda_{qr} \\ i_{ds} \\ i_{qs} \\ i_{dr} \\ i_{qr} \end{bmatrix}}_{X^{(0)}} + \underbrace{\left[\begin{array}{c|c} \mathbf{I} & \mathbf{0} \\ \hline \mathbf{0} & \mathbf{0} \end{array}\right]}_{K} \cdot \begin{bmatrix} p\lambda_{ds} \\ p\lambda_{qs} \\ p\lambda_{dr} \\ p\lambda_{qr} \\ pi_{ds} \\ pi_{qs} \\ pi_{dr} \\ pi_{qr} \end{bmatrix} \tag{3}$$

$$\begin{aligned} &\left[\hat{L}_1^{(0)} + \frac{\Delta L}{2}(e^{iw_{fc}t} + e^{-iw_{fc}t})\hat{M}\right] \cdot (X^{(0)} + X^{+} + X^{-}) \\ &+ \left[(-i\omega_e)\hat{K}X^{(0)}e^{-i\omega_e t} + (-i\omega^{+})\hat{K}X^{+}e^{-i\omega^{+}t} + (-i\omega^{-})\hat{K}X^{-}e^{-i\omega^{-}t}\right] = U \cdot e^{-i\omega_e t} \end{aligned} \tag{6}$$

Then the new form of matrix L can be updated to

$$\begin{cases} \hat{L}_1 = \hat{L}_1^{(0)} + \Delta\widetilde{L}_1(t) \\ \Delta\widetilde{L}_1(t) = \Delta L_{m1}\cos(w_{fc}t)\cdot\hat{M} \\ \hat{M} = \left[\begin{array}{c|cc} \mathbf{0} & \mathbf{0} & \\ \hline \mathbf{0} & \mathbf{I} & \mathbf{I} \\ & \mathbf{I} & \mathbf{I} \end{array}\right] \end{cases} \tag{5}$$

Therefore, in the frequency domain, the complete induction machine equation under mutual inductance change can be written as (6), where "+" and "−" represent the fault component for a faulty frequency pair $60 + f_c$ and $60 - f_c$.

Then the complete solutions X^+ and X^- for a faulty frequency pair $60 + f_c$ and $60 - f_c$ are

$$\begin{cases} \left(L_1^{(0)} - i\omega^+ K\right) X^+ + \dfrac{\Delta L_{m1}}{2}\hat{M}X^{(0)} = 0 \\ \left(L_1^{(0)} - i\omega^- K\right) X^- + \dfrac{\Delta L_{m1}}{2}\hat{M}X^{(0)} = 0 \end{cases} \tag{7}$$

where $X^{(0)}$ is the solution of

$$\left(L_1^{(0)} - i\omega_e K\right) X^{(0)} + \frac{\Delta L_{m1}}{2}\hat{M}X^{(0)} = U \tag{8}$$

Since the faulty stator current that can be measured is contained in the state variable matrix X, and matrix $(L_1(0) - i\omega^{\pm}K)$ is invertible under the context of induction machines, thus the corresponding rows of the stator current in matrix $(L_1(0) - i\omega^{\pm}K)^{-1}MX^{(0)}$ can be extracted as A^+ and A^- for frequencies ω^+ and ω^- specified in the model.

Since ΔL_{m1} is a scalar, the following results can be obtained as

$$\begin{cases} |\Delta I^+| = |A^+|\cdot\dfrac{\Delta L_{m1}}{2} \\ |\Delta I^-| = |A^-|\cdot\dfrac{\Delta L_{m1}}{2} \end{cases} \tag{9}$$

in which $|\Delta I^+|$ and $|\Delta I^-|$ are the magnitudes of the faulty stator current for a faulty frequency pair $60 + f_c$ and $60 - f_c$. The next stage task is to extract the values of $|\Delta I^+|$ and $|\Delta I^-|$ to the best possible accuracy via a variety of signal processing techniques to estimate the mutual inductance variation ΔL_m.

IV. Signal Processing Techniques

A. Challenges

Unfortunately, accurately extracting the faulty stator current at the bearing fault characteristic frequencies is not simple, as there are several technical challenges that affect the performance of conventional signal processing techniques.

1) Irrational fault frequency f_c: The bearing characteristic fault frequency f_c depends on both the bearing geometry and the motor speed ω_r, which can be an arbitrary value for mains-fed induction machines depending on the load condition. Moreover, it is almost certain that the fault frequency f_c is not an integer, but rather an irrational number. As a result, the most commonly used Fast Fourier Transform (FFT) cannot be readily used, as the FFT window length (number of sampling points) need to be adjusted to be an integer multiple of f_c, otherwise the accurate values of this frequency component cannot be extracted. A preliminary study shows the error can be well over 30% if the FFT window length is not selected, even if the window length is sufficiently long.

2) Proximity to the fundamental frequency f_s: When FFT or band-pass filtering is used to extract the faulty current, the accuracy of which would suffer if the bearing fault frequency f_c is very small, i.e., only a few Hz, so the resultant first-order faulty current frequency component $|f_s \pm f_c|$ would be very close to the fundamental frequency f_s. An example would be when the bearing fault type is inner race to cage fault, and the motor speed is low, i.e., a few hundred rpms. In addition, the faulty current component is generally 30 to 50 dB lower compared to the fundamental current, which further increases its chance of disturbance. Although this large current spike at f_s can be filtered out with analog notch filters prior to ADC, this would still add components to the existing system.

3) Real-time implementation: Although for many applications it would be acceptable to perform a bearing fault detection during an extended period of time, i.e., one to a few hours. It would be desirable if the proposed signal processing technique is able to reveal accurate faulty current components in a real-time manner, and thus the bearing fault can be also monitored in real-time, which would be beneficial for some safety-critical applications, i.e., the electric vehicles.

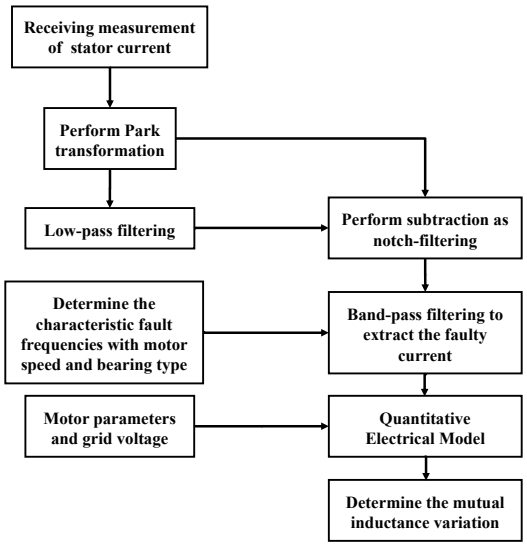

Fig. 2. Proposed signal processing technique for extracting the sum of the stator current component of the faulty frequency pairs for estimating the mutual inductance variation.

B. The Proposed Method

Taking the above challenges into consideration, an alternative approach based on "software-based notch filtering" is proposed in Fig. 2. While there exists many other signal processing techniques that may fulfill the same purpose, i.e., the compressive sensing [16], it is believed the proposed method is simple, accurate, and can be readily embedded in a controllers or DSPs for real-time monitoring.

In Fig. 2, a flow diagram is shown that extracts the input faulty current, which is then fed into the Quantitative Electrical Model for estimating the mutual inductance variation ΔL_m. The proposed method takes direct measurements of stator current in a time domain, and for an induction machine with n phases, only $n-1$ phase current measurements are required, since the additional phase current can be calculated with Kirchhoff's current law. Then the Park Transformation is applied on the measured stator currents to obtain the direct and quadrature axis current in the synchronous reference frame with a rotation speed $\omega_c = \omega_s$, and thus the largest fundamental AC component in the stator current is transformed into a DC value, which can be easily filtered out from the resultant direct and quadrature currents by performing low-pass filtering and subtraction, a process that is defined as "software-based notch filtering". The algorithm then determines the set of characteristic fault frequency pairs using bearing geometry data and real-time motor speed. Then the multiple fault frequency pairs are selected as the passband frequencies to design multiple band-pass filters to extract the faulty current from the current signals. Eventually, the root-sum-of-squres of the direct and quadrature axis currents is calculated that represents the final input faulty current to be evaluated by the Quantitative Electrical Model to determine the mutual inductance variation.

After taking the Park transformation, the frequencies of the bearing fault frequency pairs would be transformed to $|\pm f_c|$ from $|f_s \pm f_c|$, and thus the final extracted faulty current after band-pass filtering would approximately be the superposition of the faulty current magnitude $|\Delta I^+|$ at $|f_s+f_c|$ and $|\Delta I^-|$ at $|f_s-f_c|$ before the transformation. Therefore, a new expression for estimating the mutual inductance variation ΔL_m can be derived from (9) as

$$\Delta L_m = 2\frac{|\Delta I^+| + |\Delta I^-|}{|A^+| + |A^-|} \tag{10}$$

where $|\Delta I^+| + |\Delta I^-|$ is the direct output of the extracted faulty current with the proposed signal processing technique.

V. Transfer Function II

The mechanism that the air gap radial vibrations create harmonic components in the stator current is modeled as an analytical development in [17]. The motivation of Transfer Function II is to transform the mutual inductance variation profile into air gap displacement. The form of Transfer Function II is exemplified in the subfigures of Fig. 3. In the time domain, the air gap permeance, which is proportional to the mutual inductance, can be defined as the following form with the presence of a bearing fault as

$$\Lambda(t) = \Lambda_0 \frac{1}{1 - [c_0 + \sum_{k=1}^{n} c_k \cos(2k\pi f_c t)]} \tag{11}$$

where f_c is the characteristic bearing fault frequency, n is the order of the Fourier series and c_k is the coefficient, as known as ΔL_{mk}, which is obtained from the Quantitative Electrical Model by taking the extracted k^{th} order faulty current as input.

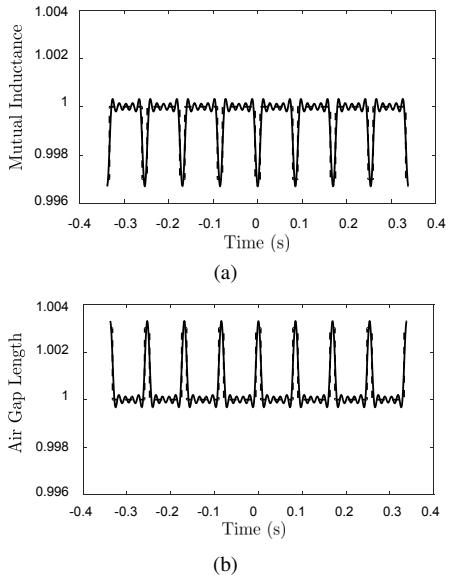

Fig. 3. Exemplar plots for (a) the reconstructed normalized mutual inductance profile in the time domain and (b) calculating the normalized air gap length profile in the time domain by taking the reciprocal of (a).

With the new mechanism proposed here, the mutual inductance profile can be reconstructed with Fourier Series terms up to the n^{th} order cosine functions and with frequencies up to $n \cdot f_c$, while their amplitudes are determined by the faulty stator current of corresponding frequencies through the Quantitative Electrical Model. In this manner, the width and shape of the mechanical vibration pulses can be reconstructed with pure electrical stator current information.

As shown in Fig. 3(a), the periodic variations of mutual inductance are triggered by the periodic air gap displacement, which is originated from the impacts of the bearing defects to other rotating parts of the bearing. This waveform can be viewed as a pulse-train pattern in the time domain, and the centers of the adjacent pulses are $1/f_c$ apart, where f_c is the characteristic bearing fault frequency. Then the air gap length profile in the time domain, as shown in Fig. 3(b), can be calculated by simply taking the reciprocal of (11) as

$$g(t) = \frac{\mu}{\Lambda(t)} = g_0\{1 - [c_0 + \Sigma_{k=1}^{n} c_k \cos(2k\pi f_c t)]\} \tag{12}$$

where μ is the air permeability, and the maximum normalized displacement of air gap length is the maximum value of $[c_0 + \Sigma_{k=1}^{n} c_k \cos(2k\pi f_c t)]$, which is also defined as the maximum bearing fault severity.

With the inclusion of higher order harmonic contents, the cumulative mutual inductance variation in the time domain can be estimated with an improved accuracy, and the reciprocal of which, the air gap length variation, defined as the bearing fault severity, can be also estimated with better accuracy.

VI. Simulation Validation

A. Validation of the Quantitative Electrical Model

An inner race to cage fault is simulated on a 6022-ZZ bearing mounted on a 5-hp induction machine running at

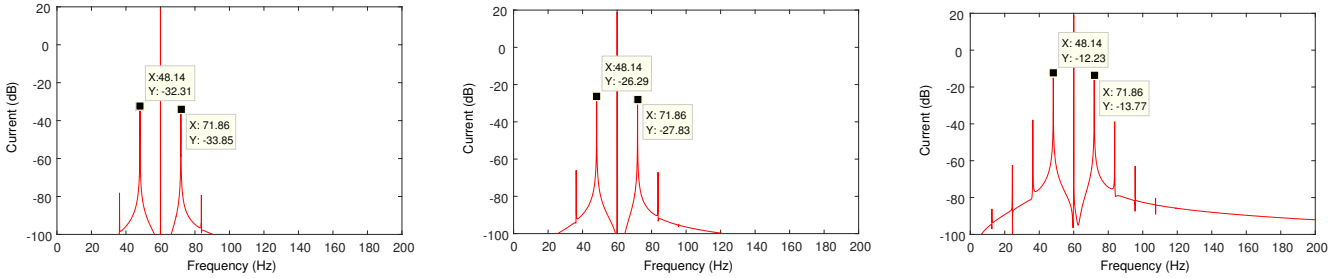

(a) (b) (c)

Fig. 4. Simulation results of the faulty current response with (a) 1% L_m variation, (b) 2% L_m variation and (c) 10% L_m variation.

TABLE I
COMPARISON OF THE STATOR CURRENT RESPONSE FROM SIMULATION AND QUANTITATIVE ELECTRICAL MODEL.

Case Number	Current Amplitude from Simulation (Reference) [A]	Current Amplitude from Analytical Model [A]	I^- % Error	I^+ % Error
Case 1: 1%	$[I^{-*}; I^{+*}]$ = [0.0305; 0.0273]	$[I^-; I^+]$ = [0.0302; 0.0255]	-0.7%	-6.6%
Case 2: 2%	$[I^{-*}; I^{+*}]$ = [0.0609; 0.0530]	$[I^-; I^+]$ = [0.0605; 0.0510]	-0.7%	-3.8%
Case 3: 10%	$[I^{-*}; I^{+*}]$ = [0.3044; 0.2573]	$[I^-; I^+]$ = [0.3023; 0.2548]	-0.1%	-1.0%

TABLE II
EXPERIMENTAL VALIDATION WITH BEARING FAULT DATASETS.

Dataset	Description	Fault Freq.	Air Gap Vibration	Estimated Air Gap Vibration	Error
Dataset F1	Electrolytic corrosion, 90% load	$f_o = 95.5$ Hz $f_i = 144$ Hz	1.23 1.43	1.15 1.54	-6.5% 7.7%
Dataset F2	Electrolytic corrosion, 90% load	$f_o = 95.5$ Hz	0.73	0.66	-9%
Dataset F3	Contaminated particle, no load	$f_i = 144$ Hz	1.33	1.26	-5.3%

1,780 rpm. The corresponding characteristic bearing fault frequency f_c is equal to 11.86 Hz, and thus the resultant first order stator current response consists of a frequency pair at 48.14 Hz and 71.86 Hz. Three bearing fault severities are modeled with different amplitudes of mutual inductance variation, namely 1%, 2% and 10%, and the stator current FFT spectral plots obtained from simulation are demonstrated in Fig. 4. These faulty conditions are also imported to the developed quantitative electrical model and the comparison results of the magnitudes of the faulty current pairs I^+ and I^- are displayed in TABLE I. The close agreement of the comparison results can validate the accuracy of the proposed model, as the maximum error is around 6%.

In addition, it is worthwhile to mention that the three subfigures of Fig. 4 are only shown for explanatory purposes, demonstrating the faulty current magnitude would be intensified with an increase in bearing fault severity. Moreover, the simulation reference values of the stator current pair are extracted when the FFT window length is deliberately selected as the integer multiple of the electrical fault frequency $|f_s \pm f_c|$, in other words, the accurate values of I^- and I^+ cannot be identified in a single FFT plot under most scenarios.

B. Validation of the Proposed Signal Processing Technique

To demonstrate the effectiveness of the proposed signal processing technique, an accelerated simulation is performed on bearing degradation, and the resultant mutual inductance variation is estimated after extracting the sum of the faulty current pairs and applying equation (10). Fig. 5 demonstrates the dynamic degradation process starting from 1 %, and then experience some step changes to 2% and 10%. Again, the close agreement observed between the reference maximum mutual inductance variation rate to the estimated value, wherein the maximum error is only around 2%, successfully verified the effectiveness of the proposed quantitative electrical model and the "software-based notch filtering" technique.

VII. EXPERIMENTAL RESULTS

As shown in Fig. 6, an experimental setup is established with an 1-hp induction machine with an air gap length of 0.28 mm and two 6022-ZZ bearings mounted on the load side and the opposite side respectively. The bearing fault on the load side 6022-ZZ is created by either contaminating the bearing with powders consisting of tiny particles [18] or through electrolytic corrosion, while the opposite side bearing is kept healthy. To validate the proposed bearing fault quantification methodology via air gap displacement, two accelerometers are

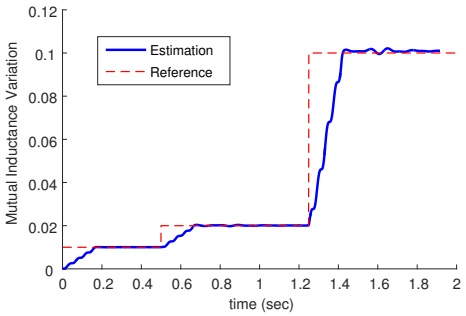

Fig. 5. Comparison of the reference and the estimated mutual inductance variation with accelerated aging study of the rolling-element bearing.

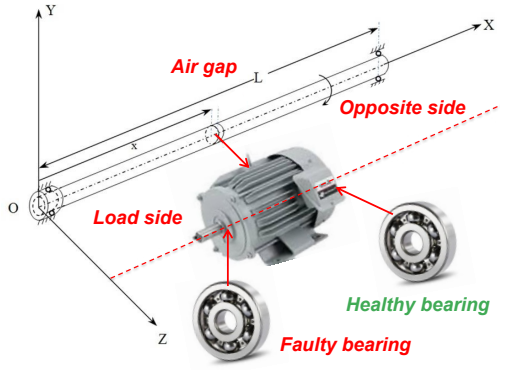

Fig. 6. Experimental setup with vibration sensors mounted close to the bearings on both the load side and the opposite side.

installed close to the bearings on both sides of the motor caps to measured the real-time vibration signals. Three datasets are collected with synchronization of the stator current and bearing vibration measurements. Since the motor shaft is considered rigid, a simple linear vibration decay model will be used to calculate the reference air gap vibration based on the two acceleration measurements transformed to displacement on both the load side and the opposite side, considering the distances between the air gap center to the two sensor mounting positions, respectively.

To validate the accuracy of the proposed bearing fault quantification model, stator current measurements from the three faulty bearing datasets are taken as the input to the proposed model, and the model output, which is the estimated air gap displacement, is compared against the benchmark air gap displacement calculated with the measured bearing vibrations using the linear vibration decay model. The complete results are summarized in TABLE II, where the largest discrepancy of the proposed quantification model for bearing fault severity is below 10%.

VIII. Conclusion

In this paper, a new vision for fault-severity based bearing fault detection is proposed, and its preliminary form of estimating the bearing fault severity in terms of radial air gap displacement is developed. The method is based on a developed analytical model of an induction machine with bearing faults that describes a relationship between the variations of mutual inductance induced by the bearing faults and the corresponding changes of stator current. The cumulative mutual inductance variation profile in the time domain can then be reconstructed with Fourier series, and the amplitudes of which are determined by the faulty current through the proposed analytical model. Later, a transfer function is adopted to transform the mutual inductance variation into the air gap length variation profile, which is used as a measure of the bearing fault severity in this study. The proposed mechanism is able to quantify bearing faults for induction machines with any power ratings and operating under any speeds and loads.

References

[1] M. E. H. Benbouzid, M. Vieira and C. Theys, "Induction motors' faults detection and localization using stator current advanced signal processing techniques," *IEEE Trans. Power Electron.*, vol. 14, no. 1, pp. 14–22, Jan. 1999.

[2] M. El Hachemi Benbouzid, "A review of induction motors signature analysis as a medium for faults detection," *IEEE Trans. Ind. Electron.*, vol. 47, no. 5, pp. 984–993, Oct. 2000.

[3] P. Zhang, Y. Du, T. G. Habetler and B. Lu,"A survey of condition monitoring and protection methods for medium-voltage induction motors," *IEEE Trans. Ind. Appl.*, vol. 47, no. 1, pp. 34–46, Jan./Feb. 2011.

[4] "Report of large motor reliability survey of industrial and commercial installations, Part I," IEEE Trans. Ind. Appl., vol. IA–21, no. 4, pp. 853-864, Jul./Aug. 1985.

[5] "Report of large motor reliability survey of industrial and commercial installations, Part II," *IEEE Trans. Ind. Appl.*, vol. IA–22, no. 4, pp. 865–872, Jul./Aug. 1985.

[6] "Report of large motor reliability survey of industrial and commercial installations: Part III," *IEEE Trans. Ind. Appl.*, vol. IA–23, no. 1, pp. 153158, Jan./Feb. 1987.

[7] JEMA, "On recommended interval of updating induction motors", 2000 (in Japanese).

[8] T. Harris, *Rolling Bearing Analysis*, 3rd ed. Hoboken, NJ, USA: Wiley, 1991.

[9] M. Blodt, P. Granjon, B. Raison and G. Rostaing,""Models for bearing damage detection in induction motors using stator current monitoring," *IEEE Trans. Ind. Electron.*, vol. 55, no. 4, pp. 1813–1822, Apr. 2008.

[10] B. Yazici and G. B. Kliman, "Adaptive, on line, statistical method and apparatus for motor bearing fault detection by passive motor current monitoring," U.S. Patent 5 726 905, Sep. 27, 1995.

[11] W. Xin, "A hybrid intelligent technique for induction motor condition monitoring," Ph.D. dissertation, Dept. Mech. Des. Eng., Univ. Portsmouth, Portsmouth, U.K., 2011.

[12] S. Singh, C. Q. Howard, and C. Hansen, "An extensive review of vibration modelling of rolling element bearings with localised and extended defects," *J. Sound Vib.*, vol. 357, pp. 300–330, 2015

[13] P. D. McFadden and J. D. Smith, "Model for the vibration produced by a single point defect in rolling element bearing," *J. Sound Vib.*, vol. 96, no. 1, pp. 69–82, 1984.

[14] Z. Kıral and H. Karagulle, "Vibration analysis of rolling element bearings with various defects under the action of an unbalanced force," *Mech. Syst. Signal Process.*, vol. 20, pp. 1967–1991, 2006.

[15] L. He, S. Cheng, Y. Du, R. G. Harley and T. G. Habetler, "Stator Temperature Estimation of Direct-Torque-Controlled Induction Machines via Active Flux or Torque Injection," *IEEE Trans. Ind. Electron.*, vol. 30, no. 2, pp. 888–899, Feb. 2015.

[16] D. Liu and D. Lu, "Off-the-grid compressive sensing for broken-rotor-bar fault detection in squirrel-cage induction motors", *IFAC-Papers OnLine*, vol. 48, no. 21, pp. 1451–1456, 2015.

[17] M. Ojaghi, M. Sabouri, and J. Faiz, "Analytic model for induction motors under localized bearing faults," *IEEE Trans. Energy Convers.*, vol. 32, no. 2, pp. 617–626, June 2018.

[18] M. Kanemaru, M. Tsukima, T. Miyauchi, and K. Hayashi, 'Bearing fault detection in induction machine based on stator current spectrum monitoring," *IEEJ J. Ind. Appl.*, vol. 7, no. 3, pp. 282–288, 2018.